Biosci. Biotech. Biochem., **60** (11), 1757–1763, 1996

Fractal Analysis of Aggregates Formed by Heating Dilute BSA Solutions Using Light Scattering Methods

Tomoaki HAGIWARA, Hitoshi KUMAGAI,* and Kozo NAKAMURA

Department of Applied Biological Chemistry, Division of Agriculture and Agricultural Life Sciences, The University of Tokyo, 1-1-1 Yayoi, Bunkyo-ku, Tokyo 113, Japan

Received March 7, 1996

The structure of aggregates formed by heating dilute BSA solution was analyzed with the fractal concept using light scattering methods. BSA was dissolved in HEPES buffer of pH 7.0 and acetate buffer of pH 5.1 to 0.1% and 0.001% solutions, respectively, and heated at 95°C, varying the heating time t_a. The fractal dimension D_f of the aggregate in the solution was evaluated from static light scattering experiments. The polydispersity exponent τ and the average hydrodynamic radius $\langle R_h \rangle$ of the aggregates were calculated from dynamic light scattering experiments using master curves obtained by Klein *et al.* The values of D_f and τ of heat-induced aggregates of BSA at pH 7.0 were about 2.1 and 1.5, respectively, the values of which agreed with those predicted by the reaction-limited cluster–cluster aggregation (RLCCA) model. On the other hand, D_f of heat-induced aggregates at pH 5.1 was about 1.8, which agreed with that predicted by the diffusion-limited cluster–cluster aggregation (DLCCA) model. The dependence of $\langle R_h \rangle$ for the sample of pH 7.0 on t_a was similar to that of the polystyrene colloids reported previously.

Key words: fractal; aggregate; light scattering; bovine serum albumin; cluster–cluster aggregation model

Globular proteins in aqueous solutions often aggregate upon heating. This phenomenon has been used in food preparation and food processing, *e.g.*, for making gel-type foods. The mechanism of the aggregation has been reported to be that heat-denatured protein molecules stick to each other by interactions such as hydrophobic interaction and disulfide bond formation.[1] There has been many studies that reported that the macroscopic physical properties of food composed of the aggregates, such as aggregated gels, varies with the aggregation conditions; for example, pH and ionic strength of the solvent.[2-4] However, most of the studies refer to only the correlation between the aggregation conditions and the macroscopic physical properties. The macroscopic properties such as mechanical properties of aggregated gels are considered to be closely related to the microscopic structure of the aggregates. Therefore, the correlation between the structure of aggregates, including its time evolution, and the macroscopic physical properties should be investigated for systematically understanding the behavior of the macroscopic physical properties developing through the aggregation. Nevertheless, the aggregates structure is only little understood.

Recently, fractal analysis has attracted attention as a quantitative analytical method that can characterize many kinds of disordered shape.[5] *Fractal* is a name for a self-similar structure which can be characterized by a *non-integer* dimension; the fractal dimension D_f.[5,6] Some colloid aggregation experiments with a technique such as light scattering and transmission electron microscopy have shown that the aggregate structure can be characterized as a kind of fractal; the *mass-fractal*.[7-9] The fractal concept has led to considerable advances in our understanding of the colloid aggregation process. With the fractal concept, several computer simulations have predicted numerically the structure and size distribution of aggregates, including the aggregation kinetics.[10-14] These predictions have been confirmed for several kinds of colloid aggregation systems.[7,8,15-17] However, there are few studies that did fractal analysis of heat-induced aggregation of protein.

In this study, before investigating the correlation between the microscopic structure of aggregates and macroscopic physical properties of foods such as aggregated gels, we investigated the fractal structure of aggregates formed by heating dilute protein solutions, by light scattering. As a material, bovine serum albumin (BSA), a typical globular protein which aggregates upon heating, was used.

Theoretical

In this section, first, we will explain the cluster–cluster aggregation model with a concept of fractal, which has been used for simulating the colloid aggregation process.[6] Second, we will explain the theory of the light scattering method for evaluating the variables in the cluster–cluster aggregation model.

Cluster–cluster aggregation.[6]

Consider diffusing particles in a certain medium. They stick to one another at contact with probability p. The resultant aggregate, what is called a cluster, can diffuse further and form larger clusters by linking to other clusters or particles. This aggregation process is called *cluster–cluster aggregation* (CCA). The CCA process is characterized by three interrelated properties: the fractal dimension of cluster D_f, the cluster mass distribution, $N(M)$, which gives the number of clusters composed of M particles, and the time dependence of the average size of clusters $\langle R \rangle$.

The fractal dimension D_f is related to the number of particles composing an aggregate, M, and the aggregate size R as[6]

* To whom correspondence should be addressed.

$$M \sim R^{D_f} \tag{1}$$

In physically realistic systems, $N(M)$ can be written as a power law type function including a cutoff function $f(x)$[6]:

$$N(M) \sim M^{-\tau} f(M/M_c) \tag{2}$$

where τ is the polydispersity exponent depending on the aggregation process, and M_c is the cutoff mass. The function $f(x)$ is approximated to be unity at $x \ll 1$, while $f(x)$ approaches zero at $x \gg 1$. As $f(x)$, an exponential function is often used[15,18,19]:

$$f(x) = \exp(-x) \tag{3}$$

As $\langle R \rangle$, the average hydrodynamic radius of aggregates, $\langle R_h \rangle$, is usually used.

Two typical CCA processes have been investigated extensively: diffusion-limited cluster–cluster aggregation (DLCCA) and reaction-limited cluster–cluster aggregation (RLCCA), corresponding to the situation of $p \approx 1$ and $p \ll 1$, respectively. By computer simulations[10-14] and aggregation experiments using such techniques as light scattering[8,7,15,16] and transmission electron microscopy,[9,17] three characteristic properties of DLCCA and RLCCA have been found; the table summarizes the three properties.

Light scattering from colloid aggregates.[20-22]

For evaluating the variables in the CCA model, two light scattering methods are used. One is static light scattering (SLS) to measure the fractal dimension D_f of the colloid aggregates. The other is dynamic light scattering (DLS) to estimate the average hydrodynamic radius of the aggregate $\langle R_h \rangle$ and the polydispersity exponent τ. Here, we will explain briefly the equations of light scattering for the fractal analysis.[20-22] The detail derivations are shown in the Appendix.

(1) Static light scattering (SLS)

In an SLS experiment, a beam of light is directed on the sample and the scattered light intensity from the sample, I, is measured as a function of the scattering vector q defined by

$$q = (4\pi n_s/\lambda)\sin(\theta/2) \tag{4}$$

where n_s, λ, θ are the refractive index of the solvent, the wavelength of the light source in a vacuum and the scattering angle (the angle between the incident and scattered beams), respectively.

The scattered intensity of a single aggregate composed of M primary particles I_M can be written as follows:

$$I_M(q) = M^2 S_M(q)(F(q))^2 \tag{5}$$

where $F(q)$ is the primary particle structure factor reflecting the structure of the primary particle, and $S_M(q)$ is the interparticle structure factor. The structure factor $F(q)$ is approximately constant if $qa_0 \ll 1$ (a_0 is the primary particle radius) as is the case for BSA (we will make sure of this assumption later). In addition, since the absolute value of $I_M(q)$ is not important, $F(q)$ will be taken as unity in this study.

Since aggregates composed of different numbers of primary particles exist together in real colloid aggregation systems, the total scattered light intensity $I(q)$ is given by

$$I(q) = \sum_M N(M) I_M(q) \tag{6}$$

At later stages in the aggregation when the $I(q)$ is entirely dominated by aggregates of $qR_g^M \gg 1$, where R_g^M denotes the radius of gyration for the aggregates, $I(q)$ is expressed as

$$I(q) \sim q^{-D_f} \tag{7}$$

(2) Dynamic light scattering (DLS)

In a DLS experiment, a beam of light is directed on the samples and the autocorrelation function of the fluctuation in the scattered light intensity from the samples, $G^{(2)}(t)$, is measured.

The variable $G^{(2)}(t, q)$ is related to the normalized electric field autocorrelation function, $g^{(1)}(t, q)$ as

$$G^{(2)}(t, q) = A(1 + \beta |g^{(1)}(t, q)|^2) \tag{8}$$

where t, A, and β are the delay time, the baseline, and a constant depending on experimental conditions, respectively. The normalized autocorrelation function $g^{(1)}(t, q)$ of the system in which the fractal aggregates of different size exist together can be written as follows:

$$g^{(1)}(t, q) = \left(\sum_M M^{2-\tau} (1 + 2q^2 (a_0 M^{1/D_f})^2 / 3D_f)^{-D_f/2} \times \exp(-M/M_c - k_B T/(6\pi\eta_s k (a_0 M^{1/D_f}))q^2 t) \right) \Big/ \left(\sum_M M^{2-\tau} (1 + 2q^2 (a_0 M^{1/D_f})^2 / 3D_f)^{-D_f/2} \exp(-M/M_c) \right) \tag{9}$$

where a_0 is the radius of the primary particles; k_B, the Boltzmann constant; T, the absolute temperature; η_s, the solvent viscosity; k, the relative value of the hydrodynamic radius of the single aggregate to its radius of gyration, which is a constant dependent on the geometry of the aggregate.[15,16,18,22,23] Next, Eq. (9) is related to $\langle R_h \rangle$ and τ.

The n-cumulant Γ_n of $g^{(1)}(t)$ is defined by[21]

$$\Gamma_n = -(\partial^n \ln(g^{(1)}(t))/\partial t^n) \quad (t \to 0) \tag{10}$$

The n-cumulant Γ_n is usually calculated by fitting the logarithm of $g^{(1)}(t)$ to a polynomial function as[21]

$$\ln(g^{(1)}(t)) \sim -\Gamma_1 t + (1/2!)\Gamma_2 t^2 - (1/3!)\Gamma_3 t^3 + (1/4!)\Gamma_4 t^4 - \cdots \tag{11}$$

From the first cumulant Γ_1, the apparent diffusion coefficient, $\langle D_{app} \rangle$, of the aggregates can be obtained[21]:

$$\langle D_{app} \rangle = \Gamma_1 / q^2 \tag{12}$$

The apparent hydrodynamic radius of the aggregates is

Table The Characteristic Properties of DLCCA and RLCCA[6-16,19]

	Fractal dimension D_f	Cluster mass distribution $N(M) = M^{-\tau}\exp(-M/M_c)$	Time dependence of $\langle R \rangle$
DLCCA	$D_f \approx 1.8$	$\tau \approx 0$	$\langle R \rangle \sim t_a^{1/D_f}$
RLCCA	$D_f \approx 2.1$	$\tau \approx 1.5$	$\langle R \rangle \sim \exp(-Ct_a)$

t_a, aggregation time.

given by using the Einstein–Stokes equation as follows:

$$\langle R_{app}\rangle = k_B T/(6\pi\eta_s\langle D_{app}\rangle) \quad (13)$$

The true average hydrodynamic radius can be expressed by[22]

$$\langle R_h\rangle = \langle R_{app}\rangle(q=0) \quad (14)$$

To calculate $\langle R_h\rangle$ from experiments, two methods are used. One is linear extrapolation of $\langle R_{app}\rangle$ to $q=0$ according to Eq. (14) (hereafter, referred to as the extrapolation method). This method is simple, however, at a later stage in the aggregation so that the $I(q)$ is entirely dominated by aggregates of $qR_g^M > 1$, satisfactory extrapolation is difficult due to the polydispersity effect.[16] The other is a master curve fitting proposed by Klein *et al.*[22] (hereafter, referred to as the master curve method). This method can evaluate $\langle R_h\rangle$ even at late stages in the aggregation, and estimate τ simultaneously. We explain the master curve method in the following paragraph.

If the aggregate is fractal and $N(M)$ can be written as the power law type function shown in Eq. (2), $\langle D_{app}\rangle/\langle D\rangle$ is a function of $q\langle R_h\rangle$ only,[22] where $\langle D\rangle$ is the average translational diffusion coefficient defined by

$$\langle D\rangle = \langle D_{app}\rangle(q=0) = k_B T/6\pi\eta_s\langle R_h\rangle .$$

That is, all experimental results at all scattering vector q and at any aggregation time t_a should fall on the single master curve $\langle D_{app}\rangle/\langle D\rangle$ *vs.* $q\langle R_h\rangle$ at each τ and D_f. Klein *et al.*[22] calculated numerically the master curves of $D_f = 2.1$ and $D_f = 1.8$, using Eq. (15) derived from Eqs. (9), (10), and (12):

$$\langle D_{app}\rangle = \left(\sum_M M^{2-\tau}(1+2q^2(a_0M^{1/D_f})^2/3D_f)^{-D_f/2} \times \exp(-M/M_c)k_BT/(6\pi\eta_s k a_0 M^{1/D_f})\right) \Big/ \left(\sum_M M^{2-\tau}(1+2q^2(a_0M^{1/D_f})^2/3D_f)^{-D_f/2} \times \exp(-M/M_c)\right) \quad (15)$$

The values of $\langle R_h\rangle$ can be calculated so that the plot of $\langle D_{app}\rangle/\langle D\rangle$ *vs.* $q\langle R_h\rangle$ makes a continuous curve. Next, since the shape of the master curves were sensitive to the value of τ,[22] τ can be evaluated by selecting the master curve that overlaps the plot of $\langle D_{app}\rangle/\langle D\rangle$ *vs.* $q\langle R_h\rangle$.

Materials and Methods

Sample preparation. All of the glass apparatus used for sample preparation was washed using a ultrasonic cleaner, rinsed with running Milli-Q water (millipore Co.), then acetone filtered through a 0.22-μm pore size filter (Minisart, Sartorious AG), and dried in a dust-free booth.

Solutions containing aggregates for SLS and DLS measurements were prepared mainly as follows. Bovine serum albumin (BSA; ref. 238040, Boehringer Mannheim GmbH) was dissolved in 50 mM HEPES buffer (pH 7.0, NaCl was added to make the ionic strength of the buffer 0.1 M), the BSA concentration being 0.1% (weight/weight). The BSA solutions were filtered through a 0.45-μm pore size filter (Minisart, Sartorious AG) into the glass vials. To prevent the evaporation of water, the surface of the sample was covered with 0.1 ml of silicon oil filtered through a 0.5-μm pore size filter (Millex-SR, Millipore Co.) and then the vials were closed tightly. The samples were aggregated by heating in a thermostatted bath at 95.0±0.2°C for various times and quenched by immediately cooling in a water bath at 25.0±0.1°C.

To investigate the effects of pH on the aggregate structure, the solutions containing aggregates were prepared at pH 5.1 and 95°C as follows. Bovine serum albumin was dissolved in 50 mM acetate buffer (pH 5.1, NaCl was added to make the ionic strength of the buffer 0.1 M) to make a 0.001% (weight/weight) solution, and filtered. The solutions were heated at 95.0± 0.2°C for 10 to 20 min and cooled at 25°C. Since the aggregation rate was too rapid under these aggregation conditions to do satisfactory DLS measurements, these samples were used only for SLS measurements.

Measurement of light scattering. Both SLS and DLS were done on a System 4700 (Malvern). The light source is a 30-mW helium–neon laser with wavelength of 632.8 nm (NEC Co., Ltd.). As for the samples prepared in HEPES buffer of pH 7.0, to suppress the effect of multiple light scattering, most of the samples were diluted 100 times (weight/weight) with the same buffer. In DLS measurement, only the samples heated for the early period of time were diluted 10 times since the scattered intensity was too weak to get satisfactory measurements for the analysis. The samples filled the measurement cell (round-glass type) and were set into the apparatus. All measurements were done at 25.0±0.1°C.

The viscosity and refractive index of the buffer were measured with a capillary viscometer (Kusano Kagaku Kikai, Tokyo) and an Abbe's refractometer (Atago, Tokyo), respectively.

SLS data were collected at scattering angles ranging from 20° to 140°. DLS experiments were done at the scattering angles selected between 20° and 140°.

Evaluation of D_f, $\langle R_h\rangle$, and τ of $N(M)$.

(1) Fractal dimension D_f.

From Eq. (7), D_f was evaluated by the slope of the double logarithmic plot of q *vs.* $I(q)$

(2) Average hydrodynamic radius $\langle R_h\rangle$ and polydispersity exponent τ.

The first cumulants were calculated by fitting $\ln(g^{(1)}(t))$ to a third-order polynomial function as explained before. Using Eq. (12), the data set of the apparent diffusion coefficient $\langle D_{app}\rangle$ for each heating time were calculated. From the data set of $\langle D_{app}\rangle$ at a heating time of 7 min, $\langle R_h\rangle$ was estimated by the extrapolation method. For the samples of heating time above 7 min, $\langle R_h\rangle$ (or $\langle D\rangle$) were calculated by shifting the data set of $\langle D_{app}\rangle$ so that the plot of $\langle D_{app}\rangle/\langle D\rangle$ *vs.* $q\langle R_h\rangle$ made a continuous curve. The polydispersity exponent τ was estimated by selecting the master curve which overlapped the obtained plot of $\langle D_{app}\rangle/\langle D\rangle$ *vs.* $q\langle R_h\rangle$.

Calculation of correlation function. To confirm the validity of the variables obtained above, the normalized electric field autocorrelation function $g^{(1)}(t, q)$ was calculated, using the values of D_f and τ estimated from the light scattering experiments. The right side of Eq. (9) was evaluated numerically and fitted to measured $g^{(1)}(t, q)$, taking M_c as a fitting variable. The radius of the primary particle a_0 was represented by the hydrodynamic radius of native BSA measured by DLS, considering that a heat-denatured globular protein is only partially unfolded.[1] For the value of k, the literature value was used.[24] The calculation was done on an M-880 (Hitachi) at the Computer Centre, the University of Tokyo.

Results

1. SLS measurement

In the analysis of this study, the primary particle structure factor $F(q)$ in Eq. (5) was assumed to be constant, this assumption being valid if $qa_0 \ll 1$. First, we estimated the value of qa_0. Since the size of a single BSA molecule was difficult to measure directly in the aggregated state, the hydrodynamic radius r_0' of a BSA molecule was measured in 6 M guanidine hydrochloride, a strong denaturant reagent, by DLS. The value of r_0' was measured to be 6.3 nm, resulting in $qr_0' \leq 0.157$ for the experimentally available value of q. A heat-denatured globular protein is only partially unfolded[1] and more compact than the protein in the presence of a denaturant such as guanidine hydrochloride.[25] Therefore, $F(q)$ will be taken as a constant in this study.

Figure 1 shows the double logarithmic plots of $I(q)$ *vs.* q for the samples prepared at pH 7.0 (a) and 5.1 (b). In Fig. 1(a), the plot approached a straight line asymptotically with increases of heating time. For the sample with a heating

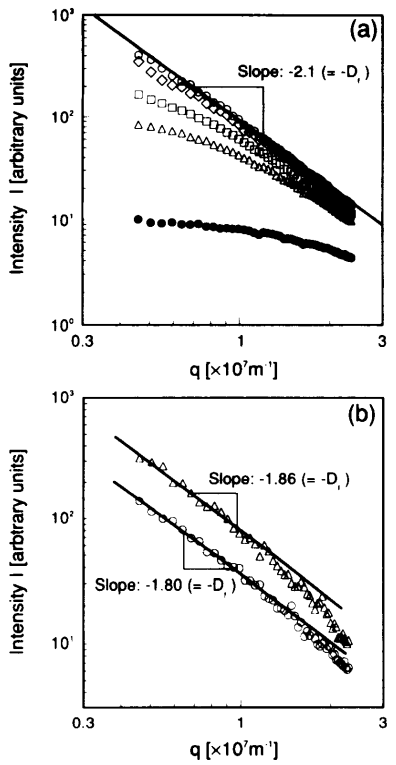

Fig. 1. Dependence of Scattered Light Intensities I of BSA Solutions Heated for Various Times t_a on q.

(a) Solvent; 50 mM HEPES buffer (pH 7.0, ionic strength = 0.1 [M]). Heating time: ●, 7 min; △, 20 min; □, 30 min; ◇, 70 min; ○, 90 min. (b) Solvent; 50 mM acetate buffer (pH 5.1, ionic strength = 0.1 [M]). Heating time: ○, 10 min; △, 20 min.

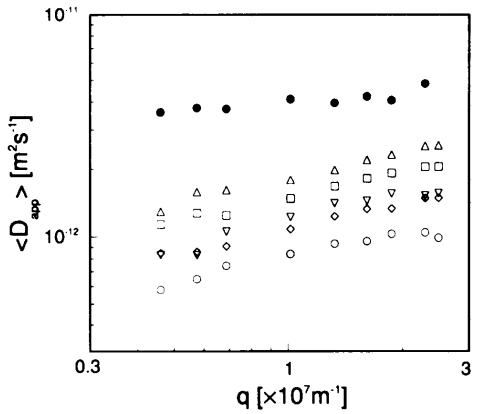

Fig. 2. Dependence of Apparent Diffusion Coefficients $\langle D_{app} \rangle$ for the BSA Aggregates in 50 mM HEPES Buffer of pH 7.0 on q.

Heating time: ●, 7 min; △, 20 min; □, 30 min; ▽, 50 min; ◇, 70 min; ○, 90 min.

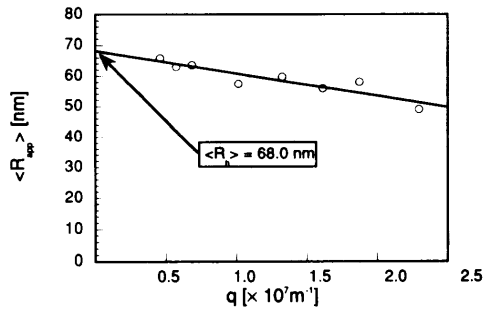

Fig. 3. Plot of $\langle R_{app} \rangle$ *vs.* q for Estimating the Average Hydrodynamic Radius $\langle R_h \rangle$.

Heating time of the sample was 7 min.

time of 90 min, the plot was a straight line because the aggregates size were large enough, as reported for such aggregates as silica and gold colloid.[7,22] From the plot with heating time of 90 min, the value of the fractal dimension D_f was 2.11 ± 0.03, which agreed with the reported value predicted by the RLCCA model, $D_f \approx 2.1$ (Table).[6,12] Figure 1(b) shows the plots of the samples prepared in the solution of pH 5.1, D_f obtained from the slope taking the value predicted by the DLCCA model, 1.80,[6,9] For the plot with heating time of 20 min, the data points were not fitted by the solid line at q over approximately $10^7\,m^{-1}$, suggesting that the aggregates were reconstructed, as reported by Aubert and Cannell[26] for the silica colloid aggregates of $D_f = 1.75 \pm 0.05$.

2. *DLS measurement*

Since the aggregation rate for the samples of pH 5.1 was too rapid, DLS measurements were done only for the samples prepared at pH 7.0 as stated before.

Figure 2 shows the plot of $\langle D_{app} \rangle$ *vs.* q. From the data of heating time 7 min, $\langle R_{app} \rangle$ was calculated by Eq. (13) and plotted against q in Fig. 3. As shown in Fig. 3, $\langle R_h \rangle$ of the samples heated for 7 min were estimated to be 68.0 nm by extrapolating $\langle R_{app} \rangle$ to $q = 0$. As for the other samples in Fig. 2, $\langle R_h \rangle$ was evaluated by the master curve method, the result being shown in the following paragraph.

Figure 4 shows the plot of $\langle D_{app} \rangle / \langle D \rangle$ *vs.* $q\langle R_h \rangle$. The solid curves are the master curves of the aggregates of

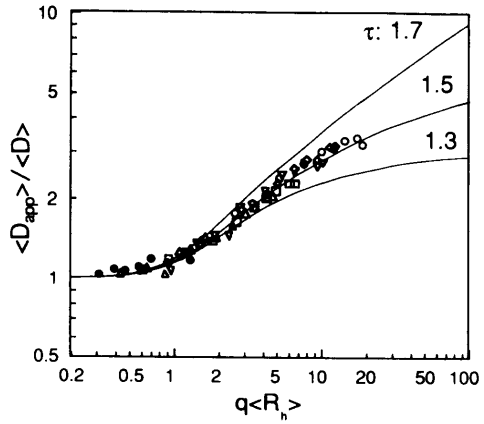

Fig. 4. Master Curve Plot of BSA Aggregates (50 mM HEPES Buffer).

Heating time: ●, 7 min; △, 20 min; □, 30 min; ▽, 50 min; ◇, 70 min; ○, 90 min. Solid curves represent the master curves of the aggregates ($D_f = 2.1$) for various value of τ, calculated by Klein *et al.* (The effect of rotational diffusion is neglected.)

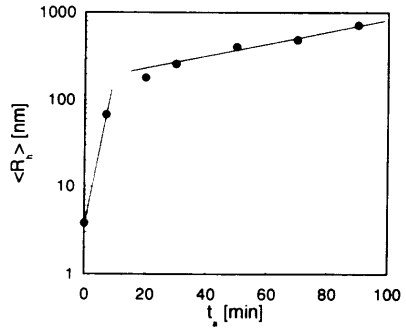

Fig. 5. The Course of the Average hydrodynamic Radius $\langle R_h \rangle$ of BSA Aggregates in 50 mM HEPES Buffer of pH 7.0.

Heating temperature was 95 C.

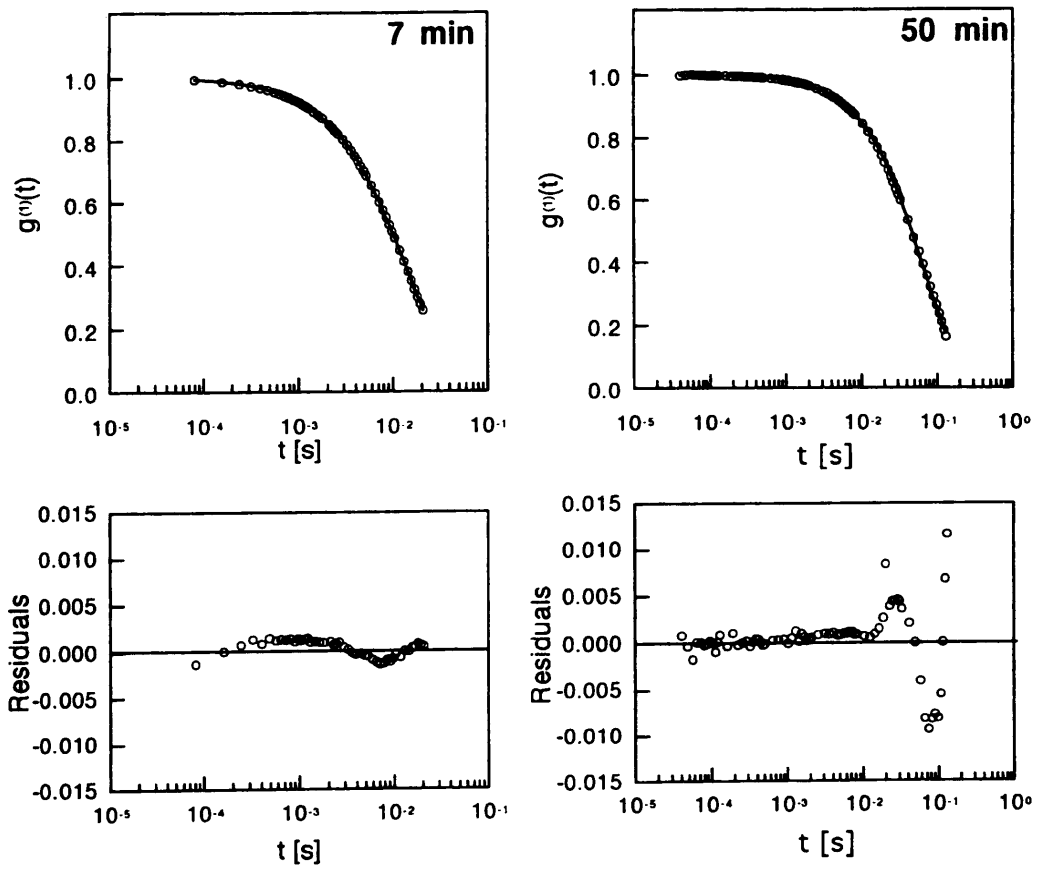

Fig. 6. The Calculated Normalized Correlation Function $g^{(1)}$.

(upper) The measured (○) and calculated (−) $g^{(1)}$. (lower) The residuals between the measured and calculated $g^{(1)}$. Samples; (left) heating time = 7 min; scattering angle, 20°; (right) heating time = 50 min; scattering angle, 20°.

$D_f = 2.1$ calculated by Klein *et al.*,[22] where the effect of the rotational diffusion was neglected. From the plot, the value of τ was estimated to be about 1.5, which agrees with the predicted value for RLCCA aggregates, $\tau \approx 1.5$.[27]

Figure 5 shows the semi-logarithmic plot of $\langle R_h \rangle$ *vs.* heating time. The plot seems to consist of two linear parts, indicating the existence of two single exponential functions across the heating time of 10 to 20 min, approximately.

3. *Calculation of correlation function*

Figure 6 shows typical calculated correlation functions $g^{(1)}(t, q)$ for heating times of 7 min and 50 min. Since the aggregation process in this study was described as RLCCA, as mentioned in Figs. 1(a) and 4, the value of k was taken as 0.97, the value in the literature for the RLCCA model.[24] The lower figures shows the residuals between the measured and the calculated $g^{(1)}(t, q)$. The calculated correlation functions $g^{(1)}(t, q)$ agreed well with those obtained from the experiments, indicating that the variables $\langle R_h \rangle$ and τ obtained were valid.

Discussion

In this study, the structure of the aggregates formed by heating BSA solutions was analyzed with a fractal concept, using light scattering methods. In particular, the fractal structure of the aggregates in the solution of pH 7.0 was precisely investigated by SLS and DLS methods, although only the SLS measurements were done for the solution of pH 5.1 due to its rapid aggregation rate.

Gimel *et al.* studied the structure and the size distribution of heat-induced aggregates of β-lactoglobulin with SLS and DLS.[19] They reported that the value of the fractal dimension D_f was 2.01 ± 0.02 which was similar to that predicted by the RLCCA model. However, in their study, the value of the polydispersity exponent τ was about 1, which disagreed with that predicted by the RLCCA model, 1.5. They did not do the heat-induced aggregation experiments at the same heating temperature and the protein concentration, probably causing this contradiction. In addition, they did not measure the course of $\langle R_h \rangle$. In this study, the experiments for the BSA solutions of pH 7.0 were done at the constant heating temperature and the constant protein concentration, and the course of $\langle R_h \rangle$ was also measured (Fig. 5). The values of D_f and τ for the BSA solutions of pH 7.0 coincided with those predicted by the RLCCA model as shown in Figs. 1(a) and 4.

As can be seen in Fig. 1, the values of D_f for the aggregates in the solution of pH 7.0 and pH 5.1 were about 2.1 and 1.8, respectively. Weitz *et al.* reported that two types of gold colloids of the fractal dimension $D_f \approx 1.8$ and 2.1 were prepared by controlling the amount of the charge on the colloid surface.[8] Lin *et al.* explained the mechanism for the gold colloid aggregates as follows[15]: If the amount of the charge on the colloid surface is reduced sufficiently, every collision results in the particles sticking, D_f taking the value of DLCCA aggregates, 1.8. On the other hand, if a large charge exists, many collisions must occur before the particles stick together due to electrostatic repulsion, D_f

taking the value of RLCCA aggregates, 2.1. The behavior of D_f for the BSA aggregates in this study can be probably explained as follows: since the isoelectric point of BSA is 4.9,[28] the amount of the average charge of BSA molecules in the solution of pH 5.1 is small enough, and D_f took the value predicted by the DLCCA model, 1.8. On the other hand, in the solution of pH 7.0, since a sufficient average charge exists on the BSA molecule, a high frequency of the collisions is necessary for the aggregation. Therefore, D_f took the value predicted by the RLCCA model.

In the RLCCA process, the course of $\langle R_h \rangle$ is described by an exponential function as explained before. On the other hand, the plot in Fig. 5 appears to consist of two single exponential functions. Lin *et al.* obtained a similar profile for the aggregation of polystyrene colloid the fractal dimension D_f and the polydispersity exponent τ of which agreed with those in the RLCCA model.[15] They supposed the reason to be as follows: the deformation of the polystyrene colloids by aggregation increases the curvature radius of the colloids.[29] Consequently, the interaction energy between two approaching particles increases, causing the decrease in aggregation rate. On the other hand, there is no clear explanation for the data in Fig. 5. However, from much research about heat-induced aggregation and gelation of globular proteins, it was shown that several interactions such as the hydrophobic interaction and disulfide bond formation take part in the linkage formation among protein molecules.[1] Furthermore, for whey protein isolate, which mainly consist of β-lactoglobulin, a globular protein, it was reported that the heat-induced gelation at pH 7.5 was caused through two steps of reaction; the linkage between protein molecules by S–S bond formation, then that by hydrophobic interaction.[30] From these aspects, it is suggested that these two-step reactions could bring about a change in interaction energy among the approaching BSA molecules during aggregation, resulting in similar time dependence of $\langle R_h \rangle$ to that of the polystyrene colloid.

In conclusion, the values of the fractal dimension D_f and the polydispersity exponent τ of heat-induced aggregates of BSA at pH 7.0 were about 2.1 and 1.5, respectively, the values of which agreed with those predicted by the RLCCA model. On the other hand, D_f of heat-induced aggregates at pH 5.1 was about 1.8, which agreed with that predicted by the DLCCA model. The course of the hydrodynamic radius $\langle R_h \rangle$ for the sample of pH 7.0 was similar to that of the polystyrene colloids reported previously.

Acknowledgments. We express our thanks to Associate Professor K. Kubota of the Department of Biological and Chemical Engineering, the Faculty of Technology, Gunma University, for his advice on light scattering experiments. Part of this work was financially supported by a Grant-in-Aid for Scientific Research from the Ministry of Education, Science, and Culture of Japan.

References

1) A. H. Clark and C. D. Lee-Tuffnell, in "Functional Properties of Food Macromolecules," ed. by J. R. Mitchell and D. A. Ledward, Elsevier Applied Science, London and New York, 1986, pp. 203–272.
2) B. Egelandsdal, *J. Food Sci.*, **45**, 570–573, 581 (1980).
3) R. K. Richardson and S. B. Ross-Murphy, *Br. Polym. J.*, **13**, 11–16 (1981).
4) H. Hatta, N. Kitabatake, and E. Doi, *Agric. Biol. Chem.*, **50**, 2083–2089 (1986).
5) B. B. Mandelbrot, "The Fractal Geometry of Nature," W. H. Freeman, San Francisco, 1982.
6) T. Vicsek, "Fractal Growth Phenomena," World Scientific, Singapore, New Jersey, London, Hong Kong, 1989.
7) D. A. Schaefer and J. E. Martin, *Phys. Rev. Lett.*, **52**, 2371–2374 (1984).
8) D. A. Weitz, J. S. Huang, M. Y. Lin, and J. Sung, *Phys. Rev. Lett.*, **54**, 1416–1419 (1985).
9) D. A. Weitz and M. Oliveria, *Phys. Rev. Lett.*, **52**, 1433–1436 (1984).
10) P. Meakin, *J. Colloid Interface Sci.*, **102**, 491–504 (1984).
11) P. Meakin, T. Vicsek, and F. Family, *Phys. Rev. B*, **31**, 564–569 (1985).
12) W. D. Brown and R. C. Ball, *J. Phys. A: Math. Gen.*, **18**, L517–L521 (1985).
13) F. Family, P. Meakin, and T. Vicsek, *J. Chem. Phys.*, **83**, 4144–4150 (1985).
14) R. Jullien, M. Kolb, and R. Botet, *J. Phys. Lett.*, **45**, L211–L216 (1984).
15) M. Y. Lin, H. M. Lindsay, D. A. Weitz, R. C. Ball, R. Klein, and P. Meakin, *Phys. Rev. A*, **41**, 2005–2020 (1990).
16) M. Y. Lin, H. M. Lindsay, D. A. Weitz, R. Klein, R. C. Ball, and P. Meakin, *J. Phys.: Condens. Matter*, **2**, 3093–3113 (1990).
17) D. A. Weitz and M. Y. Lin, *Phys. Rev. Lett.*, **57**, 2037–2040 (1986).
18) P. N. Pusey, J. G. Rarity, R. Klein, and D. A. Weitz, *Phys. Rev. Lett.*, **59**, 2122 (1987).
19) J.-C. Gimel, D. Durand, and T. Nicolai, *Macromolecules*, **27**, 583–589 (1994).
20) B. Chu, "Laser Light Scattering," 2nd Ed., Academic Press, Boston, San Diego, New York, London, Sydney, Tokyo, Toronto, 1991.
21) K. S. Schmitz, "An Introduction to Dynamic Light Scattering by Macromolecules," Academic Press, San Diego, 1990.
22) R. Klein, D. A. Weitz, M. Y. Lin, H. M. Lindsay, R. C. Ball, and P. Meakin, *Progr. Colloid Polym. Sci.*, **81**, 161–168 (1990).
23) W. Hess, H. L. Frisch, and R. Klein, *Z. Phys. B: Condens. Matter*, **64**, 65–67 (1986).
24) Z.-Y. Chen, P. Meakin, and J. M. Deutch, *Phys. Rev. Lett.*, **59**, 2121 (1987).
25) T. Koseki, N. Kitabatake, and E. Doi, *Food Hydrocolloids*, **3**, 123–134 (1989).
26) C. Aubert and D. S. Cannell, *Phys. Rev. Lett.*, **56**, 738–741 (1986).
27) R. C. Ball, D. A. Weitz, T. A. Witten, and F. Leyvraz, *Phys. Rev. Lett.*, **58**, 274–277 (1987).
28) "Concise Encyclopedia Biochemistry," 2nd Ed., ed. by T. Scott and M. Eagleson, de Gruyter, Berlin and New York, 1988, pp. 19–20.
29) R. Buscall, P. D. A. Mills, J. W. Goodwin, and D. W. Lawson, *J. Chem. Soc., Faraday Trans. 1*, **84**, 4249–4260 (1988).
30) K. Shimada and C. Cheftel, *J. Agric. Food Chem.*, **37**, 161–168 (1989).

Appendix

In the Appendix, the equations of light scattering for the fractal analysis[20–22] are derived. The second equation numbers after (A-x) correspond to those in the text.

(1) Static light scattering

The scattered intensity of a single aggregate composed of M primary particles I_M can be written as follows:

$$I_M(q) = M^2 S_M(q)(F(q))^2 \qquad \text{(A-1)(5)}$$

The variable q is the scattering vector defined by

$$q = (4\pi n_s/\lambda)\sin(\theta/2) \qquad \text{(A-2)(4)}$$

where n_s is the refractive index of the solvent; λ, the wavelength of the light source in a vacuum; θ, the scattering angle (the angle between the incident and scattered beams). The variable $F(q)$ is the primary particle structure factor reflecting the structure of primary particle. The structure factor $F(q)$ can be approximated to be unity as is shown in the text because the absolute value of $I_M(q)$ is not important. $S_M(q)$ is the interparticle structure factor. As $S_M(q)$ of fractal aggregates, the following equation is usually used:

$$S_M(q) = (1 + (2q^2(R_g^M)^2/3D_f))^{-D_f/2} \qquad \text{(A-3)}$$

where R_g^M denotes the radius of gyration for the aggregate, and D_f is the fractal dimension of the aggregates. At $qR_g^M \gg 1$, $S_M(q) \sim q^{-D_f}$.

Since the aggregates composed of different number of primary particles exist together in the real colloid aggregation system, the total scattered light intensity $I(q)$ is given by

$$I(q)=\sum_{M} N(M)I_M(q)$$

$$=\sum_{M} N(M)M^2S_M(q) \quad \text{(A-4)(6)}$$

where $N(M)$ is the cluster mass distribution which gives the number of cluster composed of M particles. At later stages in the aggregation so that the $I(q)$ is entirely dominated by aggregates of $qR_g^M \gg 1$, $I(q)$ is expressed as

$$I(q)\sim q^{-D_f} \quad \text{(A-5)(7)}$$

(2) Dynamic light scattering

The autocorrelation function of the fluctuation in the scattered light intensity $G^{(2)}(t, q)$ is related to the normalized electric field autocorrelation function, $g^{(1)}(t, q)$ as

$$G^{(2)}(t, q)=A(1+\beta|g^{(1)}(t, q)|^2) \quad \text{(A-6)(8)}$$

where t, A, and β are the delay time, the baseline, and a constant depending on experimental conditions, respectively. The normalized electric field autocorrelation function of a single aggregate composed of M particles, $g_M^{(1)}(t, q)$, can be written as follows:

$$g_M^{(1)}(t, q)=\exp(-D_{eff}^M q^2 t) \quad \text{(A-7)}$$

where D_{eff}^M is the effective diffusion coefficient of the aggregate. Both the translational diffusion and rotational diffusion of the aggregates contribute to D_{eff}^M. However, since translational diffusion mainly contribute to D_{eff}^M,[6] D_{eff}^M is approximated to the translational diffusion coefficient D_{trans}^M in this study. If aggregates of different size exist together in the system, the total normalized electric field autocorrelation function $g^{(1)}(t, q)$ is given by

$$g^{(1)}(t, q)=(1/I(q))\sum_{M} N(M)I_M(q)g_M^{(1)}(t, q)$$

$$=\left(\sum_{M} N(M)M^2S_M(q)\exp(-D_{trans}^M q^2 t)\right)\Big/\left(\sum_{M} N(M)M^2S_M(q)\right) \quad \text{(A-8)}$$

By substituting Eqs. (2) and (3) in the text, and (A-3) into (A-8), one can get

$$g^{(1)}(t, q)=\left(\sum_{M} M^{2-\tau}(1+2q^2(R_g^M)^2/3D_f)^{-D_f/2}\exp(-M/M_c-D_{trans}^M q^2 t)\right)\Big/$$

$$\left(\sum_{M} M^{2-\tau}(1+2q^2(R_g^M)^2/3D_f)^{-D_f/2}\exp(-M/M_c)\right) \quad \text{(A-9)}$$

The translational diffusion coefficient D_{trans}^M is related to the hydrodynamic radius R_h^M through the Einstein–Stokes equation as

$$D_{trans}^M=k_B T/6\pi\eta_s R_h^M \quad \text{(A-10)}$$

where k_B, T, and η_s are the Boltzmann constant, the absolute temperature, and the solvent viscosity, respectively. The relationship between R_g^M and R_h^M is given by[15,16,18,22,23]

$$R_h^M=kR_g^M \quad \text{(A-11)}$$

where k is a constant dependent on the geometry of the aggregate. The radius of gyration can be written as[15]

$$R_g^M=a_0M^{1/D_f} \quad \text{(A-12)}$$

where a_0 is the radius of the primary particles. From Eqs. (A-10) to (A-12), Eq. (A-9) can be rewritten as follows:

$$g^{(1)}(t, q)=\left(\sum_{M} M^{2-\tau}(1+2q^2(a_0M^{1/D_f})^2/3D_f)^{-D_f/2}\right.$$

$$\left.\times\exp(-M/M_c-k_B T/(6\pi\eta_s k(a_0M^{1/D_f}))q^2 t)\right)\Big/$$

$$\left(\sum_{M} M^{2-\tau}(1+2q^2(a_0M^{1/D_f})^2/3D_f)^{-D_f/2}\exp(-M/M_c)\right) \quad \text{(A-13)(9)}$$